COMPUTATION OF MAGNETIC SUSPENSION OF MAGLEV SYSTEMS USING DYNAMIC CIRCUIT THEORY

J. L. He, D. M. Rote and H. T. Coffey

Center for Transportation Research, Energy Systems Division
Argonne National Laboratory, Argonne, IL 60439, USA

ABSTRACT

Dynamic circuit theory is applied to several magnetic suspensions associated with maglev systems. These suspension systems are the loop-shaped coil guideway, the figure-eight-shaped null-flux coil guideway, and the continuous sheet guideway. Mathematical models, which can be used for the development of computer codes, are provided for each of these suspension systems. The differences and similarities of the models in using dynamic circuit theory are discussed in the paper. The paper emphasizes the transient and dynamic analysis and computer simulation of maglev systems. In general, the method discussed here can be applied to many electrodynamic suspension system design concepts. It is also suited for the computation of the performance of maglev propulsion systems. Numerical examples are presented in the paper.

INTRODUCTION

A maglev system uses three electromagnetic forces: the levitation, propulsion, and guidance forces. These forces determine the dynamic performance of the maglev vehicle. The computations of these magnetic forces may differ slightly from those in conventional electrical machines for the following reasons. First, knowledge of three-dimensional time- and space-dependent magnetic forces are required in a maglev system because the six directions of motion of a maglev vehicle are determined by these magnetic forces. Second, space harmonics, which result from the end-effect and the discontinuous distribution of the magnets aboard the vehicle, play much more important roles in the performance of a maglev vehicle. Thus, the performance analysis based on a fundamental traveling wave used in most conventional machines is inadequate. Third, transient and dynamic performance associated with vehicle motions, not steady-state performance, is emphasized in the maglev system.

Several approaches are widely used for the computation of magnetic forces in maglev systems. The finite-element method is one of the more powerful numerical techniques for solving Maxiwell's field equations. For given boundary conditions and specified system geometry, one is able to obtain sufficient information for a system by using two- and three-dimensional finite-element computer codes. However, when a system involves relative motions with space and time dependences, the finite-element method becomes difficult because a great amount of computing time is required to obtain the force-speed or force-time characteristics. In addition, most commercial finite-element computer codes that are available do not include the problems associated with moving conductors. Fourier transformation and harmonics analysis, in combination with numerical techniques, is another powerful method in maglev analysis that can be

---

used to determine the lift and drag forces in a continuous sheet guideway. The method, however, is usually limited to a two-dimensional steady-state analysis with an assumption of infinite guideway width.

The dynamic circuit theory, also called general machinery theory or mesh-matrix method, is a suitable approach for maglev applications. It can overcome some of the limitations mentioned above and can be used to perform three-dimensional electrodynamic analysis of maglev systems. The dynamic circuit theory treats an electrodynamic system in terms of space- and time-dependent circuit parameters governed by a set of differential equations in matrix form. When plate or sheet conductors are considered, the method divides the conductors into many zones, each of which carries a different current. The lumped-circuit parameters for every conducting zone are then determined, and a system of equations are formed. Once the system of equations is solved for the current distribution, the forces acting between the electrodynamic system components can be readily calculated in a straight forward manner. Therefore, the performance of the system can be investigated. Since the equations are usually solved for the currents in the time domain, the method is well suited for transient and dynamic analysis and for the computer simulation of electrodynamic systems, such as maglev trains, electromagnetic launchers, and other electrical machines. In particular, the method is currently being used at Argonne for the computer simulation of laboratory experiments, the design and analysis of maglev test facilities, and studies of conceptual maglev system designs.

Analyses of rotating electrical machines based on the general theory of electrical machines are discussed by Morgan (ref. 1). Analyses of linear machines using the mesh-matrix method have been reported (refs. 2 and 3). The dynamic circuit theory used for electromagnetic launcher analysis and simulation was discussed in several publications (refs. 4,5 and 6). As in the maglev system, the transient and dynamic performance is emphasized in electromagnetic launcher analyses. In the launcher analyses, however, a relatively short time period --a fraction of a second-- is considered because of the hypervelocity of the projectile. In addition, capacitor banks or a pulsed generator is used as the power source for electromagnetic launchers. The dynamic circuit theory used for the computation of a continuous sheet suspension was discussed by a Canadian maglev group (refs. 7 and 8). In this group's model, the dynamic circuit theory was combined with a harmonic analysis. The superconducting magnets aboard the vehicle were replaced by a current sheet that was expressed in terms of a Fourier Series. A d-q transformation, which is usually used to transform a rotating machine into a stationary primitive machine, was applied to the direction of motion for all harmonics. The performance of the continuous sheet guideway was determined on the basis of the circuit solutions in combination with the superposition theorem.

Although the dynamic circuit theory was discussed with respect to other applications in several papers, the applications of the theory to various maglev suspension and propulsion systems have not been discussed. In particular, using dynamic circuit theory to simulate the performance of a complete maglev system has not been discussed in previous papers. In this paper, we apply the dynamic circuit theory to several electrodynamic suspension systems, including a loop-shaped coil suspension, a figure-eight-shaped null-flux suspension, and a continuous sheet suspension. We also emphasize a direct computation of magnetic forces without using Fourier and d-q transformations or past computation processing. The paper provides mathematical models for various suspension systems and discusses their similarities and differences in using dynamic circuit theory. These models can be used for the development of computer codes that are necessary for the design, analysis, and

922

simulation of large-scale maglev systems. Indeed, work on the development of computer simulation codes that account for both the electrodynamics and mechanical dynamics of maglev vehicles interacting with guideways is currently in progress at Argonne.

The paper consists of seven parts. The second part introduces the dynamic circuit theory. The third part discusses the computation of magnetic forces for loop-shaped coil suspensions. The fourth part deals with the computation of figure-eight-shaped null-flux coil suspension systems. The magnetic forces in the continuous sheet-type suspension system are considered in the fifth part. Numerical examples are given in the sixth section, and conclusions are presented at the end of the paper.

GENERAL MODEL

Power Conservation and Forces in a Maglev System

A maglev system can be represented by the dynamic circuit model in which the system energy, power, and forces, as well as other quantities, are expressed in terms of their circuit parameters. Those circuit parameters, in general, are functions of time and space. Thus, the dynamic and transient performance of a maglev system can be determined on the basis of the solution of the dynamic circuit model.

In general, we may consider a maglev system in which m vehicle coils or conductors interact with n guideway coils or conductors to produce either levitation and guidance forces, or propulsion forces. All of these coils are assumed to be connected to individual power sources. Thus, the superconducting coils aboard the vehicle can be represented by letting the terminal voltages and resistances of the vehicle coils vanish, the passive guideway conductors can be represented by letting their terminal voltage vanish, and the propulsion system can be represented by connecting a polyphase power source to the guideway stator coils. If we let [i] and [e] be column (m+n) matrices made up of the individual currents and voltages associated with the vehicle and guideway coils or conductors, respectively, [L] be a square (m+n) x (m+n) matrix, each element of which represents either the self-inductances of the vehicle and guideway coils (or mutual inductance between the vehicle coils and guideway coils) and [R] be a diagonal (m+n elements) matrix composed of the individual vehicle coil and guideway coil resistances, then we can write the system voltage equations in matrix form, based on Kirchhoff's voltage law, as follows:

$$[e] = [R] [i] + \frac{d}{dt} \{ [L] [i] \}$$ (1)

We may assume that a maglev vehicle involves three-dimensional motions caused by the change of the mutual inductances between the vehicle and guideway coils in three dimensions. Letting v_x, v_y, and v_z be the velocities of the vehicle in the x, y, and z directions respectively, we can rewrite Eq. (1) in terms of a speed voltage, a voltage induced due to a relative motion, as

$$[e] = [R] [i] + v_x [G_x][i] + v_y [G_y][i] + v_z [G_z][i] + [L] \frac{d}{dt} [i]$$ (2)

where $[G_x] = d[L]/dx$, $[G_y] = d[L]/dy$, and $[G_z] = d[L]/dz$. The total time-dependent power input to a maglev system is

$$P = [i]^T[e] = [i]^T[R][i] + [i]^T[L]\frac{d}{dt}[i]$$
$$+ v_x[i]^T[G_x][i] + v_y[i]^T[G_y][i] + v_z[i]^T[G_z][i] \tag{3}$$

where the superscript T stands for the matrix transpose. Since

$$\frac{1}{2}\frac{d}{dt}\{[i]^T[L][i]\} = \frac{1}{2}v_x[i]^T[G_x][i] + \frac{1}{2}v_y[i]^T[G_y][i]$$
$$+ \frac{1}{2}v_z[i]^T[G_z][i] + [i]^T[L]\frac{d}{dt}[i] \tag{4}$$

Eq. (3) can be rewritten as follows

$$P = [i]^T[e] = [i]^T[R][i] + \frac{d}{dt}\left\{\frac{1}{2}[i]^T[L][i]\right\}$$
$$+ \frac{1}{2}v_x[i]^T[G_x][i] + \frac{1}{2}v_y[i]^T[G_y][i] + \frac{1}{2}v_z[i]^T[G_z][i] \tag{5}$$

Equation (5) shows the power conservation of a maglev system. We note in Eq. (5) that the term on the left represents the total electrical power input to the system, which may include the power from a stationary power system and the power from the batteries aboard the vehicle. The first term on the right-hand side represents the dissipated power of the system, which may include the power losses both in the guideway coils and in the vehicle coils if superconducting magnets are not used aboard the vehicle. The second term represents the time rate of change of the magnetic energy stored in the system, and the last three terms on the right-hand side represent the converted mechanical power which results in the three-dimensional motion of the vehicle. Finally, the three force components F_x, F_y, and F_y acting on the vehicle can be obtained from Eq. (5) by dividing the terms of the converted mechanical power by their corresponding velocity components v_x, v_y, and v_z, yielding the following:

$$F_x = \frac{1}{2}[i]^T[G_x][i] \tag{6}$$

$$F_y = \frac{1}{2}[i]^T[G_y][i] \tag{7}$$

$$F_z = \frac{1}{2}[i]^T[G_z][i] \tag{8}$$

According to the conventional notation, we may refer to F_x as the force in the direction of motion, which could be a propulsion force or a magnetic drag force, depending on the applications of the model, F_y in the horizontal direction, which could be a guidance or a horizontal perturbation force, and F_z in the vertical direction, which represents a levitation or a vertical perturbation force.

When the model is used to determine the magnetic drag of an EDS maglev system, the input electrical power term in the right-hand side of Eq. (5) is zero. Assuming a vehicle moving in the x direction with a speed v_x and neglecting the

induced voltage due to the horizontal and vertical perturbation, we obtain a new power conservation equation from Eq. (5) as follows:

$$[i]^T[R][i] + \frac{d}{dt}\left\{\frac{1}{2}[i]^T[L][i]\right\} + \frac{1}{2}v_x[i]^T[G_x][i] = 0 \tag{9}$$

In this case, the third term on the right-hand side represents the mechanical power required by the system to overcome the magnetic drag power of the system. Thus, the longitudinal component of the magnetic force of a maglev system can be obtained from Eq. (9) as follows:

$$F_x = \frac{1}{2}[i]^T[G_x][i] = -\frac{1}{v_x}[i]^T[R][i] - \frac{d}{dx}\left\{\frac{1}{2}[i]^T[L][i]\right\} \tag{10}$$

Equation (10) shows that the longitudinal component of the magnetic force consists of two parts. The first part is a dissipative term that represents a drag due to the ohmic loss, and the second part is due to the change of the magnetic energy stored. The second part of the force is considered to be a nondissipative or conservative force that may be negative or positive, depending on the change of the magnetic energy stored in the system in the direction of motion.

Transformation for the Coil Connections

A maglev system usually involves many coils that may logically be connected in several different groups to perform different functions, such as levitation, guidance, and propulsion. For instance, the figure-eight-shaped null-flux coil guideway can be viewed as two loop-shaped coils connected in opposite direction, and the propulsion coils, in general, are connected into three groups to form three-phase armature windings. Other maglev systems are expected to have even more complicated coil connections in order to perform an integrated maglev function. The dynamic circuit model can be applied to many maglev systems, if the transformation of the coil connections are considered.

General transformations for solving electrical machine problems were discussed by Morgan (ref 1). The transformation for the coil connections is particularly useful for the maglev simulation and analysis on the basis of the dynamic circuit model. Since the vehicle and guideway coils are usually connected in different configurations that may need different transformations, it is necessary to partition all the matrices by rows or columns to form submatrices. Thus, the previously defined current and voltage matrices expressed in terms of submatrices are

$$[i] = \begin{bmatrix} I_v \\ I_g \end{bmatrix} \tag{11}$$

and

$$[e] = \begin{bmatrix} E_v \\ E_g \end{bmatrix} \tag{12}$$

where I_v, I_g and E_v, E_g, are the current and voltage submatrices of the vehicle coils and guideway coils, respectively. The subscripts v and g stand for the vehicle and guideway, respectively. The inductance matrix becomes

$$[L] = \begin{bmatrix} L_v & L_{vg} \\ L_{gv} & L_g \end{bmatrix} \tag{13}$$

where the L_v and L_g are the inductance submatrices of the vehicle coils and guideway coils, respectively. $L_{vg}=L_{gv}$ are the submatrices that represent the coupling between the vehicle coils and guideway coils. They are the most important part of the system because all magnetic forces are generated from this coupling. Similarly, the resistance matrix in the system may be partitioned into submatrices R_v and R_g as follows:

$$[R] = \begin{bmatrix} R_v & 0 \\ 0 & R_g \end{bmatrix} \tag{14}$$

The R_v becomes a zero submatrix when superconducting coils are used aboard the vehicle. One can define a transformation matrix [T] as

$$[T] = \begin{bmatrix} T_v & 0 \\ 0 & T_g \end{bmatrix} \tag{15}$$

where T_v and T_g are the transformation submatrices for the vehicle coils and the guideway coils, respectively, which depend on the connection of the coils. T_v may be a unit submatrix if the transformation is only applied to the guideway coils. By introducing the prime quantities as a new system after transformation, one can obtain, on the basis of power invariance for the current

$$[I] = [T][I]' \tag{16}$$

and for the voltage

$$[V]' = [T]^T[V] \tag{17}$$

The inductance matrix and its derivative matrix of the new system are as follows:

$$[L]' = [T]^T[L][T] \tag{18}$$

$$[G]' = [T]^T[G][T] \tag{19}$$

$$[R]' = [T]^T[R][T] \tag{20}$$

By substituting the prime quantities in Eqs. (16) to (20) into Eqs. (1) to (10), one can obtain the power conservation and force equations for the new system. Typical examples for the use of the transformation will be discussed in the following sections.

COMPUTATION OF THE LOOP-SHAPED COIL SUSPENSION

Considerable attention has been given to suspension schemes in which the superconducting coils are levitated above a loop-shaped coil guideway, as shown in Fig. 1. The coil guideway may be superior to the continuous sheet guideway because of the former's relatively low magnetic drag force (ref. 9). The loop-shaped coil guideway, however, produces force pulsations that do not arise in the continuous-sheet guideway. A steady-state analysis of the loop-shaped coil guideway was performed by Hoppie et al. (ref. 10) on the basis of the Fourier transform method in combination with steady-state circuit analysis. The dynamic circuit model is well suited for the determination of the dynamic performance of the loop-shaped coil guideway.

When the dynamic circuit theory is applied to the loop-shaped coil guideway, the model becomes relatively simple, because the currents in the superconducting coils aboard the vehicle are usually fixed; the voltages across the individual loop coils are zero, and a connection transformation for the guideway coils is not needed. Neglecting vertical and horizontal perturbations and assuming m superconducting coils moving above n loop-shaped guideway coils, we obtain a system of voltage equations for the loop-shaped coil guideway from Eq. (2) as

$$
\begin{bmatrix} R_1 & & & \\ & R_2 & & \\ & & \cdots & \\ & & & R_n \end{bmatrix}
\begin{bmatrix} i_1 \\ i_2 \\ \cdots \\ i_n \end{bmatrix}
+
\begin{bmatrix} L_{11} & L_{12} & \cdots & L_{1n} \\ L_{21} & L_{22} & & L_{2n} \\ \cdots & \cdots & \cdots & \cdots \\ L_{n1} & \cdots & \cdots & L_{nn} \end{bmatrix}
\frac{d}{dt}
\begin{bmatrix} i_1 \\ i_2 \\ \cdots \\ i_n \end{bmatrix}
=
$$

$$
-v_x
\begin{bmatrix} G_{11} & G_{12} & \cdots & G_{1m} \\ G_{21} & G_{22} & & G_{2m} \\ \cdots & \cdots & \cdots & \cdots \\ G_{n1} & \cdots & \cdots & G_{nm} \end{bmatrix}
\begin{bmatrix} I_1 \\ I_2 \\ \cdots \\ I_m \end{bmatrix}
\tag{21}
$$

where I_j (j=1,m) are the currents in superconducting coils aboard the vehicle, L_{ij} (i=1,n and j=1,n) is the mutual inductance between the ith and j^{th} loop coils on the guideway, and R_i (i=1,n) is the resistance of the ith loop coil. Both L_{ij} and R_i are constant if the dimensions of the loop coil are selected. G_{ij} (i=1,n and j=1,m) is the derivative with respect to x of the mutual inductance between the ith loop coil on the guideway and the jth superconducting coil aboard the vehicle and is a function of space and time. The unknowns in Eq. (21) are the currents of the loop coils in the guideway. The formulas used to evaluate self-inductances and the mutual inductances can be obtained (refs.9 and 11) and the derivative of the mutual inductances can be determined numerically from the mutual inductances. Equation (21) cannot be solved directly because matrix [G] in the right-hand side is a function of time and position. One simple numerical approach is to solve Eq. (21) at successive time steps with step size Δt. Thus, for given initial conditions and determined matrix [G], one can solve Eq. (21) as a set of linear algebraic equations for the unknowns di_j/dt (j=1,n), rather than solving the linear differential equations for i_j. The currents at time t are found by adding $di_j/dt\, \Delta t$ to the previous currents, i.e.

$$\begin{bmatrix} i_1(t) \\ i_2(t) \\ \dots \\ i_n(t) \end{bmatrix} = \begin{bmatrix} i_1(t-\Delta t) \\ i_2(t-\Delta t) \\ \dots \\ i_n(t-\Delta t) \end{bmatrix} + \begin{bmatrix} di_1/dt \\ di_2/dt \\ \dots \\ di_n/dt \end{bmatrix} \Delta t \qquad (22)$$

Iterations between Eq. (21) and (22) will determine the currents in all loop coils as a function of time. The currents as a function of position are also obtained from the above results because of the relation $\Delta x = v_x \Delta t$. After finding currents in the loop coils, we are able to determine the longitudinal, the lateral guidance, and the vertical suspension forces of the system as functions of time and displacement from Eq. (6) to (8):

$$F_x = \sum_i^n \sum_j^m i_i \, G_{x,ij} I_j \qquad (23)$$

$$F_y = \sum_i^n \sum_j^m i_i \, G_{y,ij} I_j \qquad (24)$$

$$F_z = \sum_i^n \sum_j^m i_i \, G_{z,ij} I_j \qquad (25)$$

The three components of the magnetic force given by Eq. (23) to (25) include force pulsations, which depend on the geometry and the material characteristics of the loop coils. Time-average forces can be found from Eq. (23) to (25) by taking the time averages over any desired period. In practice, it is a reasonably good approximation to consider only the mutual inductances between the several coils on the left and right of a given coil. Thus, Eqs. (23) to (25), and all the mutual inductances and their derivative matrices discussed previously, are simplified. Finally, the total power dissipated in the loop coils as functions of time or position is

$$P = [\,i\,]^T [\,R\,][\,i\,] = \sum_{i=1}^n R_i \, i_i^2 \qquad (26)$$

Similarly, one can determine the time average power from Eq. (26) by taking its time average over any pulsation period.

COMPUTATION OF THE FIGURE-EIGHT-SHAPED NULL-FLUX COIL SUSPENSION

The figure-eight-shaped null-flux coil suspension and guidance system shown in Fig. 2 is a variation of the null-flux suspension concept invented by J. Powell and G. Danby in the late 1960s. It is currently being incorporated into the new Japanese maglev system[12] and has become a very important maglev concept. The major features are that it can provide both suspension and guidance forces with a relatively small magnetic

drag. In particular, it can provide zero magnetic drag at the null-flux equilibrium point and can be very helpful in starting a maglev vehicle. The Japanese have succeeded in designing and testing several versions of the electrical dynamic suspension (EDS) maglev system based on this null-flux suspension concept.

The computation of figure-eight-shaped null-flux suspensions discussed in the literatures (refs. 12 and 13) was based on field and harmonic analyses. In this section, we apply dynamic circuit theory to the figure-eight-shaped null-flux coil suspension system. As mentioned before, one of the advantages of the approach is that it can predict transient and dynamic performance based on a simple and direct solution. For general purposes, we assume that m superconducting coils interact with n figure-eight-shaped null-flux coils as shown in Fig. 3 and that the n null-flux coils comprise 2n loops. Assuming the currents in the superconducting coils are fixed and neglecting the speed voltage terms resulting from the motions in the y-z plane, we can write general voltage equations in matrix form for the 2n-loop system. Since the currents in the upper loops equal those in the lower loop but have the opposite spatial orientation, the system has only n-unknown currents, and we can apply a connection transformation to the system as discussed previously. Using Eq. (16) we can determine the transformation submatrix for the guideway coils T_g from the current relations, $i_j = -i_{n+j}$ $(j=1,n)$ as follows:

$$T_g = \begin{bmatrix} 1 & & & -1 & & \\ & 1 & & & -1 & \\ & & \ddots & & & \ddots \\ & & & 1 & & -1 \end{bmatrix}^T \tag{27}$$

Since the transformation is only applied to the guideway null-flux coils, the transformation submatrix for the vehicle coils T_v is a unit matrix. Using Eqs. (2), (15) to (20), and Eq. (27), we obtain the voltage equations in matrix form for the null-flux coil system after transformation as

$$\begin{bmatrix} R_1' & & & \\ & R_2' & & 0 \\ & & 0 & \\ & & & R_n' \end{bmatrix} \begin{bmatrix} i_1 \\ i_2 \\ \cdots \\ i_n \end{bmatrix} + \begin{bmatrix} L_{11}' & L_{12}' & \cdots & L_{1n}' \\ L_{21}' & L_{22} & & L_{2n}' \\ \cdots & \cdots & \cdots & \cdots \\ L_{n1}' & \cdots & \cdots & L_{nn}' \end{bmatrix} \frac{d}{dt} \begin{bmatrix} i_1 \\ i_2 \\ \cdots \\ i_n \end{bmatrix} =$$

$$-v_x \begin{bmatrix} G_{11}' & G_{12}' & \cdots & G_{1m}' \\ G_{21}' & G_{22}' & & G_{2m}' \\ \cdots & \cdots & \cdots & \cdots \\ G_{n1}' & \cdots & \cdots & G_{nm}' \end{bmatrix} \begin{bmatrix} I_1 \\ I_2 \\ \cdots \\ I_m \end{bmatrix} \tag{28}$$

where i_j $(j=1,n)$ is the current in the jth null-flux coil and the prime is omitted because the currents in a 2n-loop system are equal to that in an n-null-flux-coil system. The I_j $(j=1,m)$ are the currents in the superconducting coils. The individual elements in the coefficient matrices after transformation are given as follows:

$$R'_j = R_j + R_{n+j} \qquad\qquad j = 1,n \qquad\qquad (29)$$

$$L'_{ij} = (L_{ij} + L_{n+i,n+j}) - (L_{i,n+j} + L_{j,n+i}) \qquad i = 1,n \text{ and } j = 1,n \qquad (30)$$

$$G'_{ij} = G_{ij} - G_{n+i,j} \qquad\qquad i = 1,n \text{ and } j = 1,m \qquad (31)$$

where the prime quantities in the left-hand side represent the lumped-circuit parameters of the null-flux coil system. R'_j is the resistance of the jth null-flux coil, L'_{ij} is the mutual inductance between the ith and j^{th} null-flux coils, and G'_{ij} is the derivative of the mutual inductance between the ith null-flux coil and the jth superconducting coil. The right-hand side represents the parameters before transformation. Thus, R_j and R_{n+j} are the resistances in the upper and lower loops of the jth null-flux coil respectively, L_{ij} (i = 1,2n and j = 1,2n) is the self or mutual inductances between the individual loop coils, and G_{ij} and $G_{n+i,j}$ are the derivatives of the mutual inductances between the upper and the lower loop of the ith null-flux coil and the jth superconducting coil respectively. If we assume all loops of the null-flux coil to be identical, Eqs. (29) and (30) can be simplified as follows:

$$R'_j = 2R_j = 2R \qquad\qquad (32)$$

$$L'_{ij} = 2(L_{ij} - L_{i,n+j}) \qquad\qquad (33)$$

Using Eqs. (31) to (33), we can rewrite Eq. (28) in terms of the individual loop-coil parameters as follows:

$$
\begin{bmatrix} R & & & \\ & R & & \\ & & \cdots & \\ & & & R \end{bmatrix}
\begin{bmatrix} i_1 \\ i_2 \\ \cdots \\ i_n \end{bmatrix} +
\begin{bmatrix} L_{11}-L_{1,n+1} & L_{12}-L_{1,n+2} & \cdots & L_{1n}-L_{1,2n} \\ L_{21}-L_{2,n+1} & L_{22}-L_{2,n+2} & & L_{2n}-L_{2,2n} \\ \cdots & \cdots & \cdots & \cdots \\ L_{n1}-L_{n,n+1} & \cdots & \cdots & L_{nn}-L_{n,2n} \end{bmatrix}
\frac{d}{dt}
\begin{bmatrix} i_1 \\ i_2 \\ \cdots \\ i_n \end{bmatrix} =
$$

$$
-\frac{v_x}{2}
\begin{bmatrix} G_{11}-G_{n+1,1} & G_{12}-G_{n+1,2} & \cdots & G_{1m}-G_{n+1,m} \\ G_{21}-G_{n+2,1} & G_{22}-G_{n+2,2} & & G_{2m}-G_{n+2,m} \\ \cdots & \cdots & \cdots & \cdots \\ G_{n1}-G_{2n,1} & \cdots & \cdots & G_{nm}-G_{2n,m} \end{bmatrix}
\begin{bmatrix} I_1 \\ I_2 \\ \cdots \\ I_m \end{bmatrix} \qquad (34)
$$

Several important points should be noted in Eq. (34). First, the currents induced in the null-flux coils are due to the speed voltages in the right-hand side of Eq. (34). The speed voltages are given by the product of the vehicle speed v_x, superconducting coil current I_j (j=1,m), and the derivative of the mutual inductance between the moving vehicle coils and the stationary guideway coils. This means that the suspension force depends upon the product of the above three factors. Secondly, by comparing Eq. (34) with Eq. (21), one can show that the currents induced in the null-flux coil guideway are much smaller than that in the loop coil guideway for given superconducting coil currents and vehicle speeds. Equation Eq. (34) shows that for the best situation, (which assumes the

superconducting coils to be far away from the null-flux equilibrium point, that is, $L_{ij} \gg L_{n+i,j}$ and $G_{ij} \gg G_{n+i,j}$), the current induced in the null-flux coil guideway is only about one-half of that in the loop-shaped coil guideway because the speed voltage term in the right-hand side of Eq. (34) is about one-half of that of Eq. (21). From the view point of the lumped electric circuit parameters, the resistance and the self-inductance in each null-flux coil are two times larger than that in a single loop coil. In addition, the currents may be further reduced due to the reversed connection between the upper and lower loop coils which would result in a negative contribution from their mutual inductance. Both factors are observed in Eq. (34). Thus, we can conclude that the suspension forces in the null-flux coil guideway are much smaller than that in the loop-shaped coil guideway.

The three-dimensional magnetic forces, the longitudinal magnetic force F_x, the null-flux lift F_y, and the vertical guidance force F_z, are obtained from Eqs. (6) to (7), and (31) as follows:

$$F_x = \sum_{i=1}^{n} \sum_{j=1}^{m} i_i I_j \left[\frac{\partial M_{ij}}{\partial x} - \frac{\partial M_{n+i,j}}{\partial x} \right] \tag{35}$$

$$F_y = \sum_{i=1}^{n} \sum_{j=1}^{m} i_i I_j \left[\frac{\partial M_{ij}}{\partial y} - \frac{\partial M_{n+i,j}}{\partial y} \right] \tag{36}$$

$$F_z = \sum_{i=1}^{n} \sum_{j=1}^{m} i_i I_j \left[\frac{\partial M_{ij}}{\partial z} - \frac{\partial M_{n+i,j}}{\partial z} \right] \tag{37}$$

Equations (35) to (37) illustrate that all magnetic forces in the null-flux coil guideway are determined by the difference of the forces acting on the upper loop and the lower loop coils. All magnetic forces vanish at the null-flux equilibrium point, as expected.

CONTINUOUS SHEET SUSPENSION

A continuous sheet guideway is one of the basic levitation methods for electrodynamic suspension maglev systems. The repulsive levitation force is generated by the interaction between the superconducting coils aboard the vehicle and the eddy currents induced in the conducting sheet. The computation of lift and drag forces for a continuous sheet guideway is discussed in the literature (refs. 14 and 15). In particular, combining the Fourier transformation method with a numerical approach seems to be a powerful method. Most of these methods, however, neglect edge effects due to the finite width of the guideway and are based on steady state analyses.

When the dynamic circuit method is applied to a continuous sheet guideway, it divides the plate or the sheet conductors into many zones as shown in Fig. 4, each of which carries a different current. The circuit parameters for every conducting zone are then determined, and the system of equations is formed. The number of conducting zones is determined by the need for accurate computation. When the current distribution is known by solving the system of equations, the performance of the system can be calculated. When the circuit parameters are evaluated on the basis of a finite

length of the conducting zone in the y direction, the edge effect of the guideway is taken into consideration.

If we assume m superconducting magnets moving above a conducting sheet guideway which is divided into n conducting zones, we can write the voltage equations for the sheet guideway in matrix form as

$$
\begin{bmatrix} R_1 & & & \\ & R_2 & 0 & \\ & 0 & & \\ & & & R_n \end{bmatrix}\begin{bmatrix} i_1 \\ i_2 \\ \cdots \\ i_n \end{bmatrix} + \begin{bmatrix} L_{11} & L_{12} & \cdots & L_{1n} \\ L_{21} & L_{22} & & L_{2n} \\ \cdots & \cdots & \cdots & \cdots \\ L_{n1} & \cdots & \cdots & L_{nn} \end{bmatrix}\frac{d}{dt}\begin{bmatrix} i_1 \\ i_2 \\ \cdots \\ i_n \end{bmatrix} + \begin{bmatrix} V_{s1} \\ V_{s2} \\ \cdots \\ V_{sn} \end{bmatrix} =
$$

$$
- V_x \begin{bmatrix} G_{11} & G_{12} & \cdots & G_{1m} \\ G_{21} & G_{22} & & G_{2m} \\ \cdots & \cdots & \cdots & \cdots \\ G_{n1} & \cdots & \cdots & G_{nm} \end{bmatrix}\begin{bmatrix} I_1 \\ I_2 \\ \cdots \\ I_m \end{bmatrix} \tag{38}
$$

where R_i and L_{ij} (i,j=1,n) are the resistances and inductances of the conducting zones, and G_{ij} is the derivative of the mutual inductance between the ith conducting zone and the jth superconducting coil. In Eq. (38) a column voltage matrix $[V_s]$ appears which represents the unknown voltages across the finite width of the conducting sheet. We may call this a side-voltage which does not exist in either the loop-shaped coil guideway or the figure-eight-shaped coil guideway. To solve the currents induced in each conducting zone, two additional conditions must be imposed. First, the total current flowing in the conducting sheet must be zero. Second, side-voltages across all conducting zones must be equal, that is

$$
i_1 + i_2 + i_3 + \ldots + i_{n-1} + i_n = 0 \tag{39}
$$

and

$$
V_{s1} = V_{s2} = \ldots = V_{sn-1} = V_{sn} = V_s \tag{40}
$$

Thus, Eqs. (38) to (40) involve n+1 equations. For given initial current conditions, we can solve the n+1 equations as a set of coupled linear equations for n unknown current derivatives and one side-voltage V_s. The currents in the conducting zones at time t are obtained by adding di/dt Δt to the currents at t-Δt as shown in Eq. (22). Continuous iterations will determine the currents in all the conducting zones as a function of time or displacement. Following the solution of these currents, we are able to find all magnetic forces acting on the superconducting coils as given by Eqs. (6) to (8). In the continuous sheet guideway, F_x is the longitudinal magnetic force, F_y is the lateral force due to the edge effect in the finite width guideway, and F_z is the repulsive suspension force.

NUMERICAL EXAMPLES

Several computer codes for different guideway options have been developed based on the model discussed in this paper. Numerical examples are given only on the figure-eight-shaped coil suspension because of the limited length of this paper. Table 1 shows the dimensions of a superconducting coil and the null-flux coils used as numerical examples. A computer simulation is performed on a single superconducting coil

932

moving above a null-flux coil guideway with a 20-cm equivalent air-gap, as shown in Fig. 2. The time-averaged null-flux lift, magnetic longitudinal force (which equals the magnetic drag force), and the horizontal guidance force are shown as functions of the vertical displacement in Fig. 5. This figure shows that, as expected, all time-averaged forces disappear at the null-flux equilibrium point, and that they are symmetrical about the axis y=0. Fig. 6 shows the time-averaged forces as a function of vehicle speed from which one can see that the lift-to-drag ratio is about 20 at a high speed, and that a drag peak appears at 20 m/s. This implies that the dimensions of the null-flux coils may be optimized; for instance, the resistance of the null-flux coil may be reduced. Two options may be considered for the reduction of the coil resistance: one is to increase the cross-section of the aluminum coils, and the other is to use a copper conductor for the null-flux coil guideway.

Force fluctuations associated with the null-flux coil guideway are shown in Fig. 7, which shows that all forces fluctuate around their average values. Typical fluctuations for the null-flux lift and the horizontal guidance forces are about 10%. The frequency of the fluctuations is determined by the vehicle speed divided by the average length of the null-flux coil. Thus, for v=67 m/s and a coil length of 0.55 m, the frequency is 122 Hz.

Table 1 Dimensions of Superconducting Coils and Null-flux Coils

Superconducting coil
length	1.5	m
width	0.5	m
current	550	kA-T

Figure-eight-shaped null-flux coils
length	0.5	m
height/loop	0.35	m
gap between upper and lower loops	0.05	m
gap between null-flux coil	0.05	m
cross-section	9	cm^2
material	aluminum	
Equivalent Air gap	20	cm

CONCLUSION

Dynamic circuit theory, as applied to the maglev problem, treats all magnetic forces acting between components of a maglev system as arising from changes in magnetic energy stored in that system. This paper shows that mathematical models based upon this theory can be readily constructed to represent moving vehicle magnets interacting with stationary conductor arrays distributed on a guideway. Models of three types of guideway conductors were considered in order to demonstrate the utility and versatility of the approach. Very general expressions were given for the forces between vehicle and guideway components for all three types of guideway conductors. This showed that, in general, single-loop conductors provide larger lift force than null-flux loop conductors. Numerical results of computer codes based on the mathematical model of a null-flux loop guideway conductor array were also given. In conclusion, the dynamic circuit theory provides a powerful approach to analyzing complex and heretofore difficult to handle problems involved in maglev system design.

REFERENCES

1. Morgan, A. T.:   General Theory of Electrical Machines. Heyden & Son Ltd., London, 1979.

2. Elliott, D. G.:   Matrix Analysis of Linear Induction Machines. Final Report prepared for FRA, Dept. of Transportation, Office of Research and Development, Washington, D.C. 20590, Sept., 1975.

3. Ooi, B. T.:   A generalized Machine Theory to the Linear Motor. IEEE Trans. Power Apparatus and Systems, Vol. PAS-92, No. 5, July/Aug. 1973, pp. 1252-1259.

4. He, J. L; Levi, E.; Zabar, Z. and Birenbaum, L.:   Concerning the Design of Capacitively Driven Induction Coil Guns. IEEE Trans. on Plasma Science, Vol. 17, No. 3, June 1989, pp. 429-438.

5. He, J. L; Zabar, Z.; Levi, E. and Birenbaum, L.:   Transient Performance of Linear Induction Launchers Fed by Generators and by Capacitor Banks. IEEE Trans. on Magnetics, Vol. 27, No. 1, Jan. 1991. pp. 585-590.

6. Elliott, D. G.:   Mesh-Matrix Analysis Method for Electromagnetic Launchers. Fourth Symposium on Electromagnetic Launch Technology, Austin, Texas, April 12-14, 1988.

7. Ooi, B. T.:   A Dynamic Circuit Theory of the Repulsive Magnetic Levitation System. IEEE Trans. Power Apparatus and System, Vol. PAS-96, No. 4, July/Aug. 1977, pp. 1094-1100.

8. Jain, O. P.:   Further Applications of the Dynamic Circuit Theory to the Electrodynamic Repulsive Magnetic Levitation Systems. Ph.D. Dissertation, Department of Electrical Engineering, McGill University, Montreal, Canada, July 1978

9. Nasar, S. A. and Boldea, I.:   Linear Electric Motors: Theory, Design, and Practical Applications. Prentice-Hall, Inc., Englewood Cliffs, N. J., 1987.

10. Hoppie, L. O.; Chilton, F.; Coffey,H. T. and Singleton, R. S.:   Electromagnetic Lift and Drag Force on a Superconducting Magnet Propelled along a Guideway Composed of Metallic Loops. Proc. of Applied Superconducting Conf., May 1-3, 1722, Annapolis, Maryland, IEEE Pub. No. 72CH0682-5-TABSC.

11. Grover, F. W.:   Inductance Calculations Working Formulas and Tables. Dover Publications, Inc., New York, 1962.

12. Fujiwara, S.; and Fujimoto, T.:   Characteristics of the Combined Levitation and Guidance System Using Ground Coils on the Side Wall of the Guideway. International Conf. Maglev '89, July 1989, pp. 241-244.

13. Saitoh, T.; Miyashita, K.; and Kiwaki, H.:   Study for Harmonic Ripple of Electromagnetic Force in Superconducting Magnetically Levitated Vehicle with Non-Rectangular Ground Coils. International Conf. Maglev'89, July 1989, pp. 245-250.

14. Coffey, H. T.; Chilton, F.; and Hoppie, L. O.: The Feasibility of Magnetically Levitating High Speed Ground Vehicles, prepared by Stanford Research Institute for U. S. Dept. of Transportation, FRA, Report FRA-10001, Feb. 1972.

15. Reitz, J. R.; and Davis, L. C.:   Force on Rectangular Coil Moving above a Conducting Slab. Journal of Applied Physics, 43(4), April 1972, pp. 1547-1553.
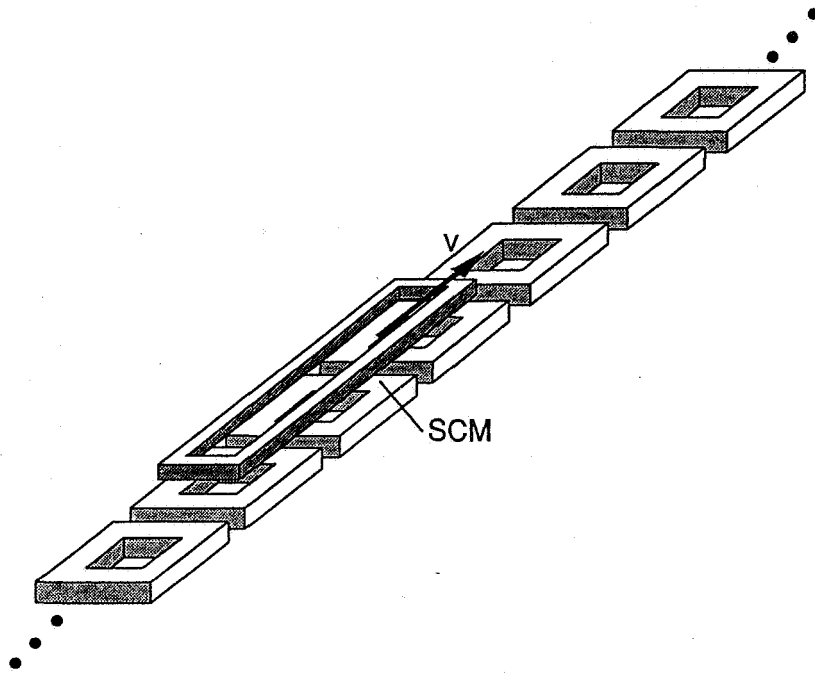
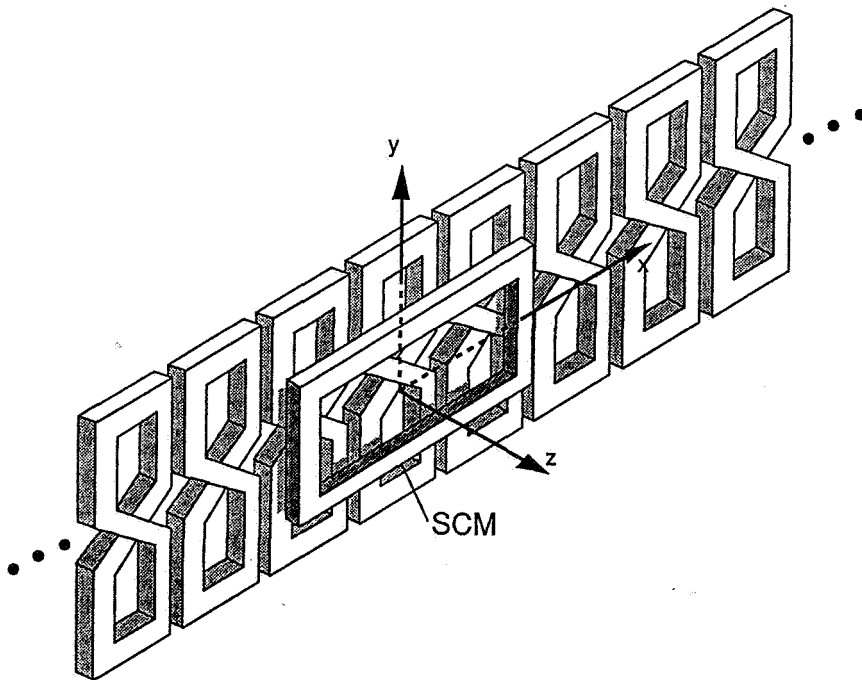Fig. 1   A Sketch of Loop-shaped Coil Suspension

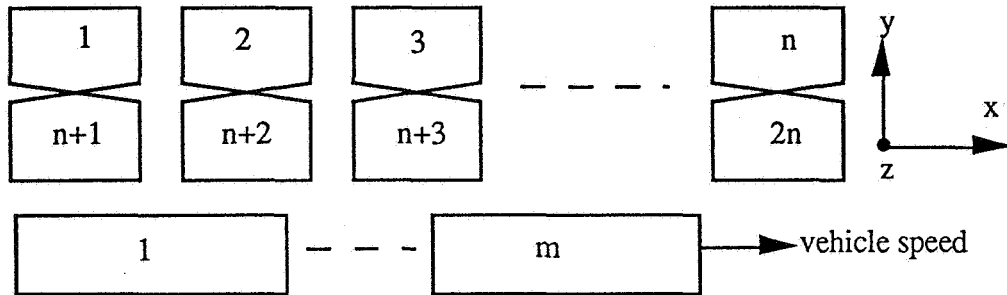Fig. 2   A Sketch of Figure-Eight-Shaped Coil Suspension

Fig. 3 Dynamic Circuit Application to the Figure-Eight-Shaped
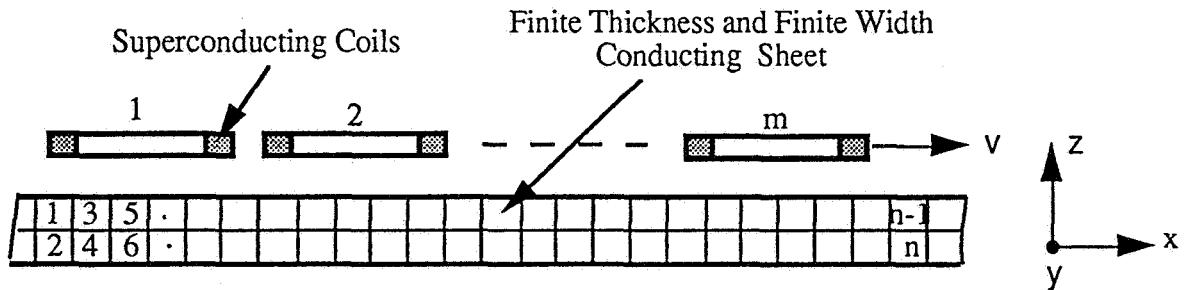Null-Flux Coil Suspension

Fig. 4 Dynamic Circuit Theory Application to the Finite Thickness
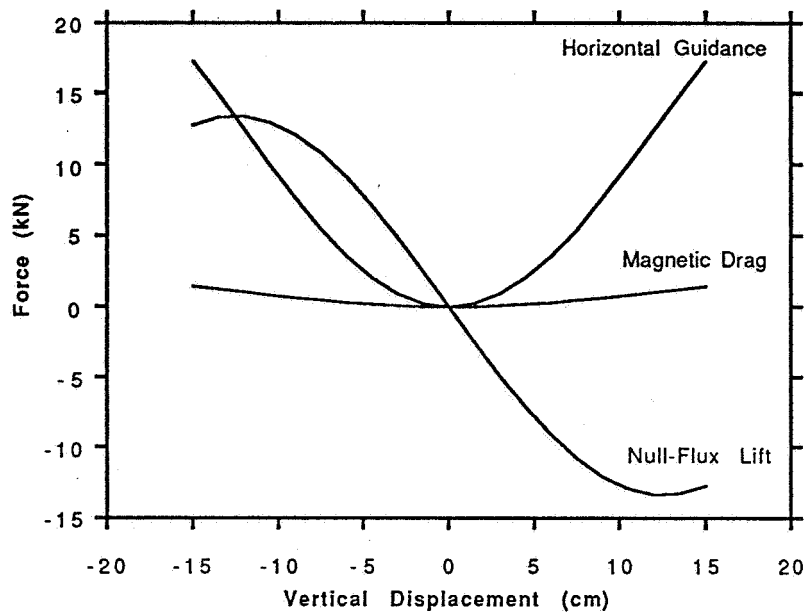and Finite Width Continuous Sheet Guideway

Fig. 5   Time-Averaged Null-Flux Lift, Magnetic Drag, and Horizontal Guidance
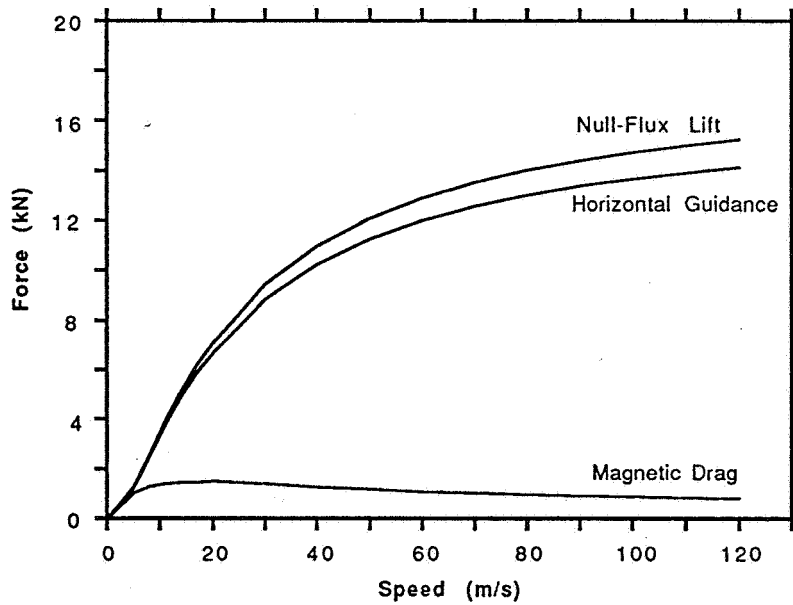Forces vs. Vertical Displacement with a Vehicle Speed of 67 m/s

Fig. 6   Time-Averaged Null-Flux Lift, Magnetic Drag, and Horizontal Guidance
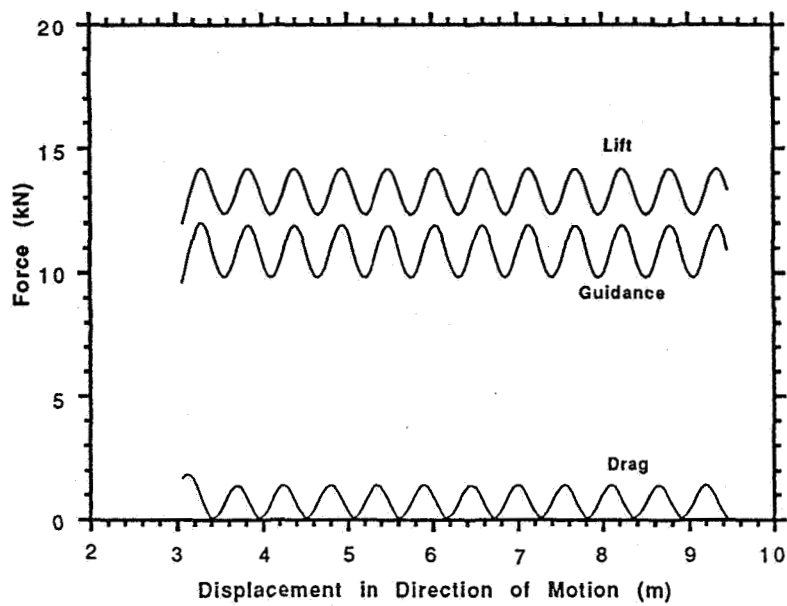Forces vs. Vehicle Speed with 11-cm Vertical Offset

937

Fig. 7   Force Pulsations in Null-Flux Coil Suspension System